Unique Properties of *Plasmodium falciparum* Porphobilinogen Deaminase*[S]

Viswanathan Arun Nagaraj[‡], **Rajavel Arumugam**[‡], **Bulusu Gopalakrishnan**[§], **Yeleswarapu Sri Jyothsna**[§], **Pundi N. Rangarajan**[‡], **and Govindarajan Padmanaban**[‡1]

From the [‡]Department of Biochemistry, Indian Institute of Science, Bangalore 560012, India and the [§]Life Sciences Division, Innovation Labs Hyderabad, Tata Consultancy Services, Hyderabad 500081, India

The hybrid pathway for heme biosynthesis in the malarial parasite proposes the involvement of parasite genome-coded enzymes of the pathway localized in different compartments such as apicoplast, mitochondria, and cytosol. However, knowledge on the functionality and localization of many of these enzymes is not available. In this study, we demonstrate that porphobilinogen deaminase encoded by the *Plasmodium falciparum* genome (PfPBGD) has several unique biochemical properties. Studies carried out with PfPBGD partially purified from parasite membrane fraction, as well as recombinant PfPBGD lacking N-terminal 64 amino acids expressed and purified from *Escherichia coli* cells (ΔPfPBGD), indicate that both the proteins are catalytically active. Surprisingly, PfPBGD catalyzes the conversion of porphobilinogen to uroporphyrinogen III (UROGEN III), indicating that it also possesses uroporphyrinogen III synthase (UROS) activity, catalyzing the next step. This obviates the necessity to have a separate gene for UROS that has not been so far annotated in the parasite genome. Interestingly, ΔPfPBGD gives rise to UROGEN III even after heat treatment, although UROS from other sources is known to be heat-sensitive. Based on the analysis of active site residues, a ΔPfPBGDL116K mutant enzyme was created and the specific activity of this recombinant mutant enzyme is 5-fold higher than ΔPfPBGD. More interestingly, ΔPfPBGDL116K catalyzes the formation of uroporphyrinogen I (UROGEN I) in addition to UROGEN III, indicating that with increased PBGD activity the UROS activity of PBGD may perhaps become rate-limiting, thus leading to non-enzymatic cyclization of preuroporphyrinogen to UROGEN I. PfPBGD is localized to the apicoplast and is catalytically very inefficient compared with the host red cell enzyme.

Detailed studies of the metabolic pathways in the malarial parasite hold promise for the identification of new antimalarial drug targets (1, 2). Earlier studies in this laboratory had shown that the malarial parasite synthesizes heme *de novo*, despite acquiring heme from the host red cell hemoglobin in the intraerythrocytic stage. It has been shown that *Plasmodium falciparum* contains δ-aminolevulinate dehydratase (ALAD)[2] of dual origin: one species encoded by the parasite genome (PfALAD) and another imported from the host red cell. Inhibition of ALAD activity in the parasite, the second enzyme of the pathway with a specific inhibitor, succinylacetone, leads to inhibition of heme synthesis and death of the parasite, indicating the potential of the pathway as a drug target (3, 4).

Heme biosynthesis from glycine and succinyl-CoA involves eight different steps and the genes for all the enzymes of the pathway, with the exception of uroporphyrinogen III synthase (UROS, *hemD*) have been located on the parasite genome (5). However, a *hemD* orthologue has been identified in *Toxoplasma gondii* and is expected to be targeted to the apicoplast, a chloroplast-like organelle in the parasite (6). Based mostly on bioinformatics-based predictions, some experimental data and hypothesis, a hybrid model for heme biosynthesis has been proposed. The model involves shuttling of intermediates of the pathway between mitochondria, apicoplast, and cytoplasm and the localization of the Pf enzymes in the different compartments (6–9). However, experimental evidence for the functionality of the Pf enzymes in the parasite, and their actual site of localization is available only in a few cases. Sato and Wilson (10) have shown that PfALAD is functional. Sato *et al.* (7) have also shown that PfALA synthase (ALAS) and PfALAD are targeted to the mitochondrion and apicoplast, respectively, based on transfection studies in *P. falciparum* cultures involving GFP fusion constructs. Studies in this laboratory have shown that PfALAS is active and the native enzyme is localized to the parasite mitochondrion (11). PfALAD and Pf ferrochelatase (PfFC) are also functional, and the native enzymes are localized to the apicoplast (12, 13). However, it has been pointed out as unpublished data (9) that in PfFC-GFP fusion gene-transfected parasites, the protein is targeted to the mitochondrion.

In the light of the dual origin of the enzymes of the heme-biosynthetic pathway in the parasite (12–14), it is of importance to establish the functionality of the Pf enzymes. A difficulty has been to express adequate quantities of recombinant Pf enzymes, perhaps due to the hydrophobic N-terminal targeting sequence, AT-rich codon bias and recovery of recombinant

[2] The abbreviations used are: ALAD, δ-aminolevulinate dehydratase; ALAS, δ-aminolevulinate synthase; PBGD, porphobilinogen deaminase; UROS, uroporphyrinogen III synthase; FC, ferrochelatase; UROGEN, uroporphyrinogen; URO, uroporphyrin; ΔPfPBGD, recombinant parasite genome-coded PBGD lacking N-terminal 64 amino acids; PBS, phosphate-buffered saline; GFP, green fluorescent protein.

proteins from the inclusion bodies. This laboratory has been able to overcome these limitations by expressing the truncated proteins without the hydrophobic targeting sequence, using *E. coli* Rosetta strain 2(DE3)pLysS that has seven tRNAs for rare codons permitting universal translation and working out the optimal conditions for expressing the recombinant proteins in the cytosol. In the present study, the unique features of parasite genome-coded porphobilinogen deaminase (PfPBGD) are described. Surprisingly, the recombinant enzyme lacking the N-terminal hydrophobic sequence (ΔPfPBGD) is able to catalyze the formation of UROGEN III, even after heat treatment, rather than UROGEN I that is derived from pre-uroporphyrinogen in the absence of UROS, thus obviating the necessity for a separate PfUROS. All the properties of the recombinant enzyme including formation of UROGEN III, are also shown by the native enzyme in the parasite. Sato *et al.* (7) have shown that the N-terminal sequence of PfPBGD directs the reporter GFP to the apicoplast in fusion gene-transfected parasites. The present study reveals that the native PfPBGD is indeed localized to the apicoplast. The enzyme is catalytically very inefficient, when compared with the host red cell enzyme.

EXPERIMENTAL PROCEDURES

Parasite Maintenance and Isolation—*P. falciparum* culture was maintained on human O^+ red cells at 5% hematocrit in RPMI 1640 with glutamine (Invitrogen) supplemented with 10% O^+ human serum by the candle jar method (15). Cultures were synchronized by sorbitol treatment (16), and the parasites usually at the trophozoite stage were isolated by treatment with equal volumes of 0.15% (w/v) saponin (17). The released parasites were pelleted down and washed four times with ice-cold phosphate-buffered saline. The final wash was free of detectable hemoglobin.

Cloning, Expression, and Purification of ΔPfPBGD cDNA— The full-length PfPBGD could not be expressed in *E. coli* Rosetta2(DE3)pLysS strain, but it was possible to express PfP-BGD lacking 64 N-terminal amino acids (ΔPfPBGD). Again, the protein expressed using pRSETA plasmid (Invitrogen) did not bind to the Ni^{2+}-NTA column under non-denaturing conditions, but the species expressed with C-terminal histidine tag using pET-20b(+) plasmid (Invitrogen) bound to Ni^{2+}-NTA column and could be purified. The 1.1-kb cDNA (Fig. 1*A*) obtained using the primers, 5′-GACCGGATCCGGGAACTC-GTGATTCTCCG-3′ and 5′-ACCCTCGAGTTATTTATTA-TTTAAAAGGTGCAATTCAGCCT-3′, based on the nucleotide sequence of putative PfPBGD gene sequence (PFL0480W) described in PlasmoDB data base, was sequenced (ABI prism, 310 Genetic Analyzer) to confirm in-frame alignment of the cloned cDNA with the vector-encoded His tag as well as for the absence of PCR-based mutations.

Recombinant plasmids were transformed into *E. coli* Rosetta2(DE3)pLysS strain (Novagen), and cells were grown to an A_{600} of 1.0 at 30 °C in a rotary shaker. The cells were then grown at 18 °C for 30 min, and protein expression was induced with 1 mM 1-thio-β-D-galactopyranoside for 13 h at 18 °C. The recombinant protein was recovered in both soluble (20–30%) and membrane (70–80%) fractions. The soluble enzyme with C-terminal histidine tag was purified by Ni^{2+}-NTA chroma-

tography under non-denaturing conditions. Briefly, *E. coli* cells were lysed in 50 mM Tris buffer, pH 7.5, containing 50 mM KCl, 10% glycerol, and 2 mM β-mercaptoethanol by sonication. The lysate was centrifuged at 50,000 × *g* for 1 h, and the supernatant was applied to a column packed with Ni^{2+}-NTA resin in the presence of 15 mM imidazole. The column was then washed sequentially with the lysis buffer containing 30, 50, and 75 mM imidazole and finally the ΔPfPBGD protein was eluted from the column with lysis buffer containing 300 mM imidazole and 1% Triton X-100 (Fig. 1*B*). Following dialysis against lysis buffer, the purified protein was stored at 4 °C up to one month. Host PBGD was partially purified from human erythrocytes using DEAE-cellulose and Q Sepharose as described (18, 19).

Generation of ΔPfPBGDL116K Mutant—Site-directed mutagenesis was carried out as described (20). The following primer pair carrying the required mutations was used for PCR amplification of pET-20b(+) plasmid containing ΔPfPBGD cDNA to generate the plasmid containing ΔPfPBGDL116K cDNA: 5′-GT AAG AGT GTT GGA AAA TAT GGC GGG AAA GG-3′ and 5′-CC TTT CCC GCC ATA TTT TCC AAC ACT CTT AC-3′. The mutant codons are underlined. The PCR product obtained with Phusion High Fidelity Polymerase was treated with DpnI to digest the methylated parental DNA strand, transformed into *E. coli* DH5α strain and ampicillin-resistant colonies were isolated. The plasmid containing ΔPfPBGDL116K cDNA was isolated, and the mutation was confirmed by DNA sequencing. Expression and purification of ΔPfPBGDL116K mutant protein from *E. coli* Rosetta2(DE3)pLysS was carried out essentially as described above.

Enzyme Assay—PfPBGD was assayed essentially as described by Jordan *et. al* (21) with 4 mM porphobilinogen (Sigma) in a final volume of 50 μl of 50 mM Tris, pH 7.5 containing 40 mM KCl, 0.8% Triton, 8% glycerol, and 2 mM β-mercaptoethanol. Incubation was carried out at 37 °C and higher temperatures for different periods of time. The reaction was stopped by the addition of 30 μl of 5 N HCl and porphyrinogens were oxidized to porphyrins by exposure to light for 20 min. The absorbance was measured at 405 nm against buffer blank ($E_{mM} = 548$ M^{-1} cm^{-1}). An enzyme-omitted control was included in all the assays. Host PBGD assay was carried out at pH 8.2 with 2 mM porphobilinogen under the same conditions.

HPLC Analysis for Product Characterization—HPLC analysis was carried out essentially as described by Lim *et al.* (22) with Waters HPLC system (model 515, with dual absorbance detector). Briefly, 25 μl of the assay mixture was loaded onto a C18 Sun Fire column (5 μm, 4.6 × 250 mm). The solvent system consisted of acetonitrile and 1 M ammonium acetate buffer, pH 5.16. A 15-min linear gradient elution with 13% (v/v) acetonitrile to 30% acetonitrile in ammonium acetate buffer followed by an isocratic elution at 30% acetonitrile for further 15 min was used. Standard uroporphyrin I (URO I) and III (URO III) (Frontier Scientific) were used to spike the reaction products to enable characterization of the isomer (Supplemental Fig. S1A).

Identification of Dipyrromethane Cofactor—Purified ΔPfPBGD was treated with modified Ehrlich reagent (1 g of *p*-dimethylamino benzaldehyde in 8 ml of 70% perchloric acid + 42 ml of glacial acetic acid), and the spectrum was recorded at different

intervals. The presence of dipyrromethane in the enzyme is indicated by the formation of a purple color with an absorption maximum around 555 nm within 5 min, with the color fading to an orange-yellow color in about 20 min, with a new absorption maximum around 495 nm (23).

Preparation of Parasite Membrane Fraction—PBGD enzyme activity was also assayed in parasite membrane (total organellar) fraction prepared as described by Sharma *et al.* (24). For this purpose, parasites were resuspended in 20 mM Tris (pH 7.5) containing 250 mM sucrose and sonicated for 1 min at 30% amplitude with alternative cooling. This lysate was centrifuged at 150,000 × *g* for 30 min, and the supernatant (cytosol) was removed. The pellet was solubilized in a buffer containing 50 mM Tris, pH 7.5, 50 mM KCl, 1% Triton X-100, 2 mM *β*-mercaptoethanol, and 10% glycerol. The supernatant obtained after centrifugation at 15,000 × *g* was used as solubilized membrane fraction. Marker analysis of the parasite membrane and cytosol fractions was carried out as described by Varadharajan *et al.* (13). The solubilized membrane fraction was routinely heat-treated at 80 °C for 20 min before assaying for PfPBGD activity.

Localization of PfPBGD—To study the localization of PfPBGD in *P. falciparum* the method described by Tonkin *et al.* (25) was followed. Polyclonal antibodies were raised against ΔPfPBGD in rabbit and IgG was purified using protein A Sepharose chromatography. The parasite-infected red blood cell pellet was washed thrice with phosphate-buffered saline (PBS) and then fixed with 4% paraformaldehyde (w/v) and 0.0075% glutaraldehyde (v/v) for 30 min. After washing with PBS, the fixed cells were permeabilized with 1% Triton X-100 and treated with 0.1 mg/ml (PBS) sodium borohydride for 10 min. Blocking was carried out with 3% bovine serum albumin. Rabbit anti-ΔPfPBGD IgG and mouse anti-ΔPfALAD IgG or mouse anti-PfALAS IgG were used at 1:200 dilution and incubated for 2 h. FITC-conjugated goat anti-rabbit IgG and TRITC-conjugated goat anti-mouse IgG (Santa Cruz Biotechnology) were then added and incubated for 1 h at 1:200 dilution. Cells were then allowed to settle onto poly-L-lysine coated coverslips (Sigma) and mounted in 50% glycerol with 0.1 mg/ml of 1,4-diazabicyclo[2,2,2]octane (DABCO, Sigma). Fluorescence microscope (Leica Microsystems) was used and images were acquired at ×100 magnification using an oil immersion objective and Leica FW 4000 image acquisition software.

Other Procedures—Western blot analysis of ΔPfPBGD and the parasite membrane fraction was carried out with purified IgG (1:1000 dilution) using standard procedures.

RESULTS

Purification of ΔPfPBGD—The ΔPfPBGD lacking the 64 N-terminal amino acids of PfPBGD was expressed using pET-20b(+) plasmid and purified from *E. coli* lysate by Ni^{2+}-NTA chromatography (see "Experimental Procedures"). The purified protein appeared as a doublet on SDS gel (Fig. 1*B*, *lane 6*), and the faint upper 45-kDa band may be because of the presence of the uncleaved periplasmic localization signal. The doublet (45/43 kDa) reacted with monoclonal anti-histidine tag antibody as well as anti-ΔPfPBGD IgG (Fig. 1, *C* and *D*). This recombinant enzyme designated as ΔPfPBGD, and the host enzyme partially purified from red cells were used in all subsequent studies.

Properties of ΔPfPBGD—Initial studies with recombinant enzyme purified using Ni^{2+}-NTA column did not show any activity when incubated at 37 °C for 1 h, unlike the host enzyme. Because PBGDs are known to be heat stable (21, 26), assays were carried out at higher temperatures when the enzyme activity could be detected. The optimum temperature for ΔPfPBGD was around 65 °C (Fig. 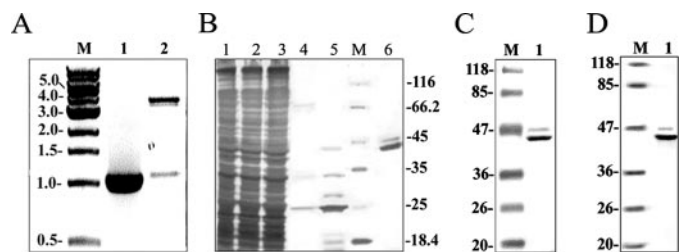2*A*). The enzyme lost very little activity even when heated to 80 °C and then assayed at 37 °C (Fig. 2*B*). The enzyme gave a typical spectrum for the presence of dipyrromethane cofactor with Ehrlich reagent (Fig. 2*C*). In view of these results, assays were carried out for prolonged periods of time at 37 °C. The enzyme activity picked up after a lag of about 2 h and was linear up to 12 h (Fig. 3*A*). The host enzyme did not show a lag and reached saturation in about 4 h (Fig. 3*D*). In general, the specific activity of the host enzyme was 25–30-fold higher than that of the ΔPfPBGD. The pH optima of ΔPfPBGD and

FIGURE 1. **Cloning and expression of truncated *P. falciparum* porphobilinogen deaminase (ΔPfPBGD).** *A*, cloning of ΔPfPBGD cDNA into *E. coli* expression vector. *Lane 1*, 1.1-kb ΔPfPBGD cDNA obtained by RT-PCR; *lane 2*, BamHI-XhoI digest of recombinant pET-20b(+) plasmid carrying ΔPfPBGD cDNA. *Lane M*, 1-kb ladder (*kb*). *B*, purification of ΔPfPBGD from *E. coli* cells by Ni^{2+}-NTA affinity chromatography. *Lane 1*, *E. coli* cell lysate; *lane 2*, flow-through fraction from Ni^{2+}-NTA column, *lanes 3–5*, washes with lysis buffer containing 30, 50, and 75 mM imidazole. *Lane 6*, heat-treated 300 mM imidazole eluate of Ni^{2+}-NTA column; *Lane M*, protein molecular weight markers (*kDa*). *C* and *D*, Western blot analysis of purified ΔPfPBGD using mouse anti-His tag antibody and rabbit anti-ΔPfPBGD IgG.
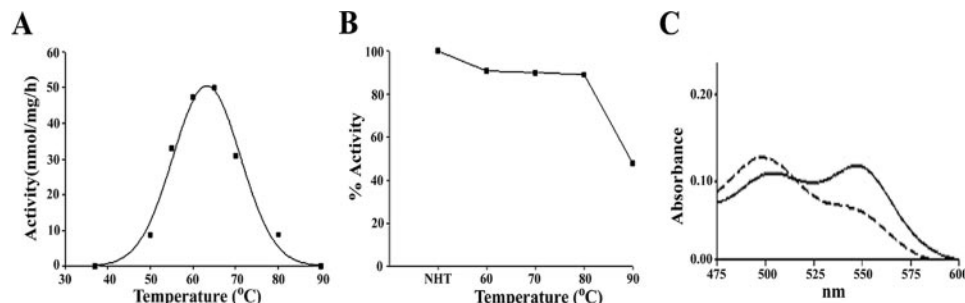

FIGURE 2. **Characteristics of ΔPfPBGD.** The enzyme was assayed by measuring the absorbance of the porphyrin product formed at 405 nm as described under "Experimental Procedures." Activity is expressed in terms of the porphyrin product formed. *A*, enzyme was incubated at the temperatures indicated for 1 h. *B*, enzyme was pretreated at the temperatures indicated for 20 min and then incubated at 37 °C for 12 h. *NHT*, non-heated control activity was taken as 100% (3.8 nmol/mg protein/h). *C*, dipyrromethane identification in the purified enzyme with modified Ehrlich reagent. *Continuous line*, spectrum taken within 5 min (peak at 555 nm); *dashed line*, spectrum taken after 20 min (peak at 495 nm).
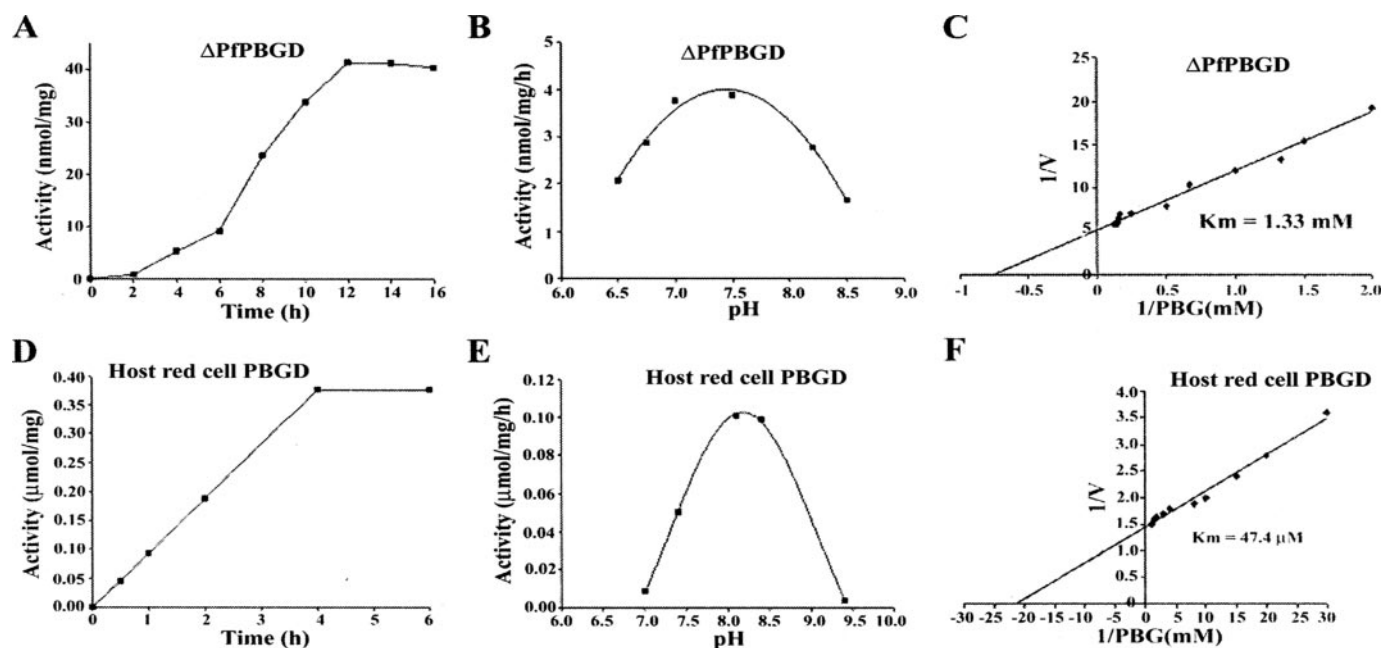
FIGURE 3. **Properties of ΔPfPBGD and host red cell PBGD.** The enzymes were assayed under conditions described in the text. The host human red cell enzyme was partially purified and protein estimated after SDS-PAGE. The *top* and *bottom rows* depict data obtained with ΔPfPBGD and host PBGD, respectively. *A* and *D*, time course; *B* and *E*, pH optima; *C* and *F*, Lineweaver-Burk plots.
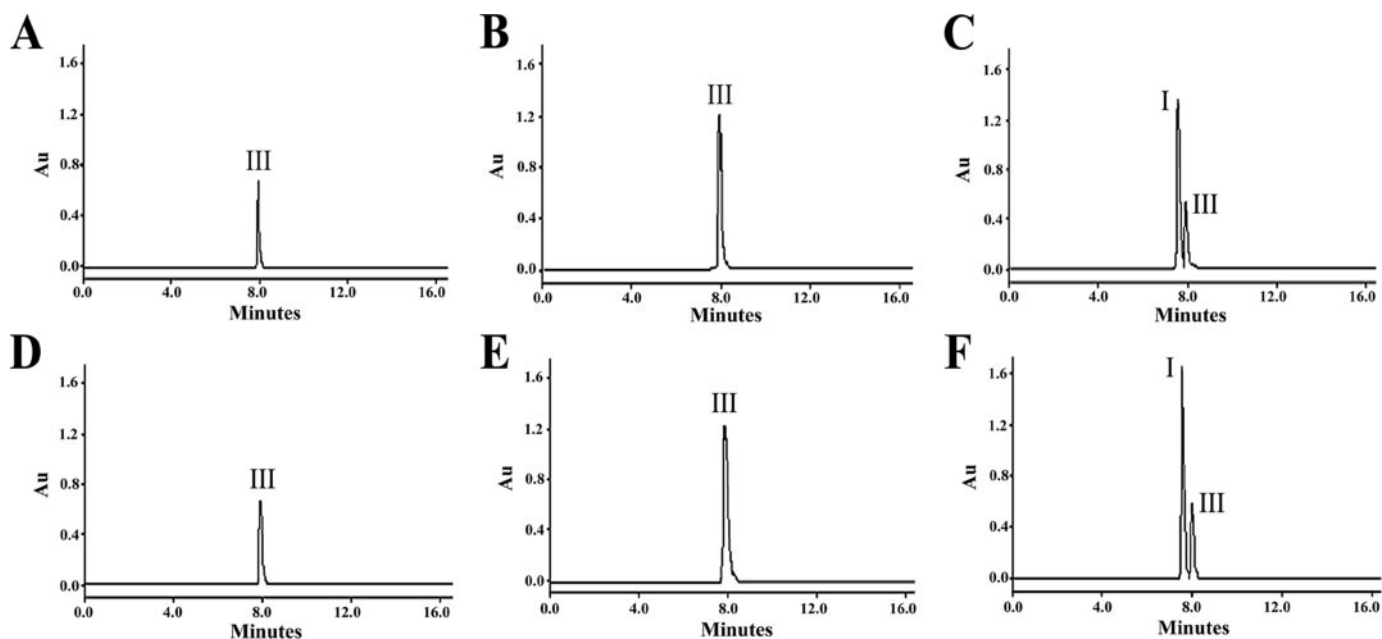

FIGURE 4. **Product characterization of ΔPfPBGD reaction.** The enzyme was incubated with the substrate for 12 h, and the porphyrin product was analyzed on HPLC column as described under "Experimental Procedures." The *top* and *bottom rows* refer to the product analysis without and with heat treatment (80 °C for 20 min) of the recombinant enzyme. *A* and *D*, HPLC profile of product; *B* and *E*, product spiked with URO III; *C* and *F*, product spiked with URO I.

host PBGDs were found to be in the ranges 7.1–7.5 and 8.1–8.4, respectively (Fig. 3, *B* and *E*). There was substantial difference in the K_m values for ΔPfPBGD (1.3 mM) and host enzyme (47.4 μM) (Fig. 3, *C* and *F*).

ΔPfPBGD Catalyzes Formation of Uroporphyrinogen III (UROGEN III)—PBGDs catalyze the formation of pre-uroporphyrinogen which spontaneously cyclizes to UROGEN I in the absence of UROS, the latter enzyme being responsible for the formation of UROGEN III due to ring D inversion (27). The UROS gene has not as yet been identified on the par-

asite genome, and this enzyme activity is essential for the normal functioning of the heme-biosynthetic pathway. Surprisingly, ΔPfPBGD was found to give rise to UROGEN III (URO III after oxidation). While spiking with standard URO III enhanced the peak height of the product, spiking with URO I gave a separate peak (Fig. 4, *A–C*). The standard method of PBGD purification involves heat inactivation of UROS, but interestingly, ΔPfPBGD gave UROGEN III even after heat treatment (Fig. 4, *D–F*). This unique property of the enzyme obviates the necessity to have a separate gene for UROS on the
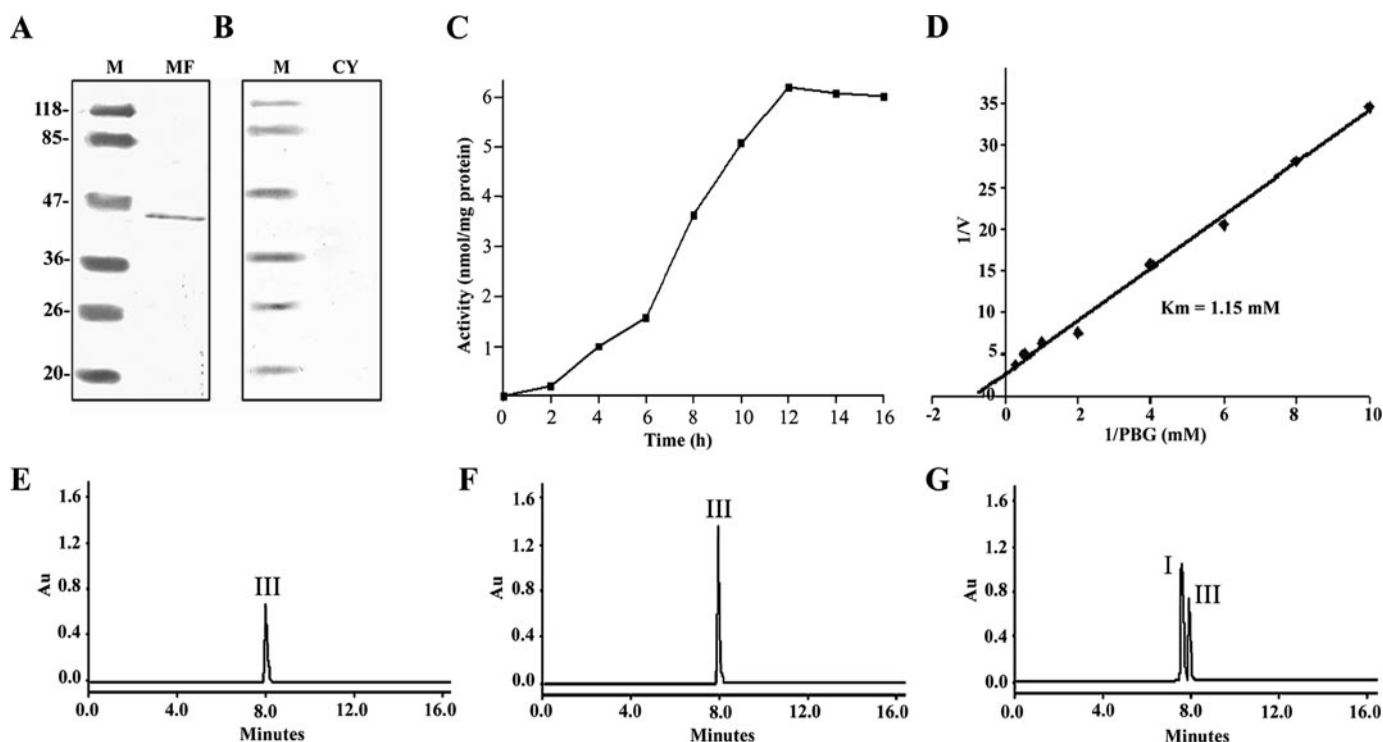
FIGURE 5. **Properties of native PBGD in the membrane fraction from *P. falciparum*.** The membrane fraction was prepared from the parasite pellet, solubilized, and heat treated as described under "Experimental Procedures" and used for the assays. *A* and *B*, Western blot analysis of the membrane and cytosolic fractions from *P. falciparum*. *M*, marker; *MF*, membrane fraction; *CY*, cytosol fraction. *C*, time course. *D*, Lineweaver-Burk plot. *E*, HPLC profile of product. *F*, product spiked with URO III. *G*, product spiked with URO I.

parasite genome. As expected, the host red cell enzyme after heat treatment gave rise to UROGEN I (URO I after oxidation) (Supplemental Fig. S1, *B–D*).

Properties of PfPBGD from the Parasite—To carry out the enzyme assay for the parasite genome-coded PBGD in *P. falciparum,* the parasite pellet was fractionated into membrane and cytosol fractions as described under "Experimental Procedures." Western blot analysis was carried out with anti-ΔPfPBGD IgG. The results presented in Fig. 5, *A* and *B* indicate that a 43-kDa protein was detected only in the membrane fraction and not in the cytosol. The total membrane pellet was solubilized as described under "Experimental Procedures," and PBGD enzyme assays were carried out after heat treatment. All the properties listed for the recombinant enzyme were also seen with the native enzyme in the parasite. The time course kinetics obtained was similar to that obtained with ΔPfPBGD (Fig. 5C). The K_m was found to be 1.15 mM (Fig. 5D). Importantly, heat-treated membrane fraction gave UROGEN III as the end product (Fig. 5, *E–G*). The pH and temperature optima were similar to that of the recombinant enzyme (data not presented).

To rule out the outside possibility of the presence of an independent heat-stable PfUROS in the parasite membrane extract and contribution of inadequately inactivated *E. coli* proteins as contaminants in the purified recombinant PfPBGD to UROS activity, the following control experiments were carried out: The parasite membrane extract was immunoprecipitated with anti-ΔPfPBGD IgG, and the supernatant was assayed for PBGD and UROS activities and neither activity could be detected. The supernatant was also added to partially purified host PBGD to look for UROS activity. The *E. coli* Rosetta strain, transformed

with pET-20b(+) without PfPBGD-cDNA, was assayed for UROS activity after heat denaturation of the extract, as such and in the presence of host PBGD. In all these experiments only URO I was detected as the product of the reaction, and there was no evidence for the formation of URO III. These results rule out any extraneous contribution to the bifunctional character of PfPBGD (data not presented). Attempts to carry out complementation studies with *E. coli hemD* mutant (28) were not successful, because PfPBGD expression required the use of the Rosetta strain, and no detectable expression could be seen in the mutant strain used.

Studies with ΔPfPBGD Mutant—A perusal of the amino acid sequence of PfPBGD (Fig. 6) reveals that it shares most of the essential amino acid residues established with PBGDs from different sources (29, 30). Thus, it shares all the 8 arginines, the mutation of which leads to a decrease in activity. In particular, the parasite enzyme manifests the conserved motif VGTSSL followed by arginines 131 and 132 in *E. coli*. (It is IGTSSL followed by arginines 216 and 217 in the parasite.) It also shares other conserved residues such as Gln[19(75)], Phe[62(123)], Asp[84(145)], Leu[159(244)], and the active site Cys[242(359)], the numbers outside and inside the parenthesis indicating the positions in *E. coli* and parasite enzymes, respectively (31). In addition, PfPBGD shares the lysine 59 at an equivalent position, but instead of lysine 55 it has leucine 116. It has been shown that modification of one of the two conserved lysine residues leads to inactivation of PBGD in *E. coli* (32). Therefore, it was of interest to examine the contribution of leucine 116 to the low activity of the parasite enzyme by changing the leucine back to lysine, as is seen in the *E. coli* enzyme.

FIGURE 6. **Amino acid sequence alignment between PBGDs from *E. coli* and *P. falciparum*.** The alignment has been performed using the "needle" program (Needleman-Wunsch global Alignment algorithm) of the EMBOSS suite. Identity: 101/451 (22.4%), Similarity: 172/451 (38.1%), Gaps: 154/451 (34.1%). Score: 381.0. Crucial identical amino acid residues are *highlighted* and discussed in the text.
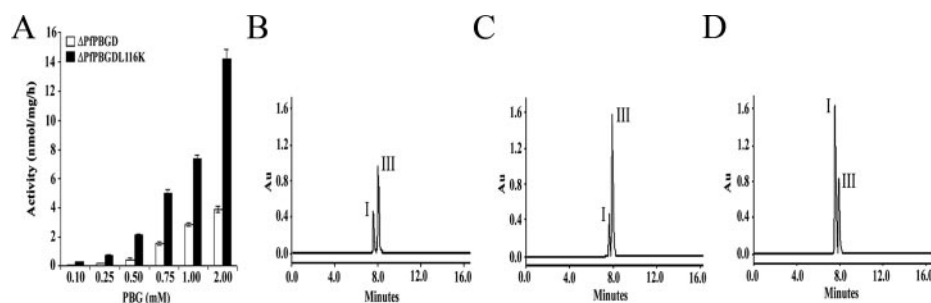

FIGURE 7. **Properties of the ΔPfPBGDL116K mutant enzyme.** The mutant enzyme was generated and purified as described under "Experimental Procedures." *A*, activity of wild-type and mutant enzymes were compared with increasing substrate concentration. *B–D*, HPLC profiles of the product as such (*B*) and after spiking with URO III (*C*) and URO I (*D*).
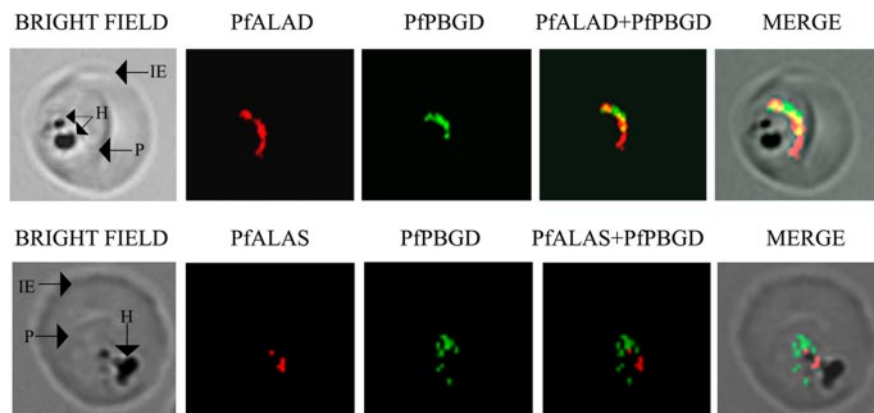

FIGURE 8. **Localization of PfPBGD with PfALAD and PfALAS in *P. falciparum* by immunofluorescence.** The experimental details are given under "Experimental Procedures." *IE*, infected erythrocyte; *P*, parasite; *H*, hemozoin.

The results obtained with ΔPfPBGDL116K indicate that the mutant enzyme has at least 5-fold higher activity than ΔPfPBGD (Fig. 7*A*). More interestingly, the product profile now indicates a significant amount of URO I along with URO III (Fig. 7, *B–D*).

Localization of PfPBGD in P. falciparum—Immunofluorescence studies were carried out to identify the localization of native PfPBGD using anti-ΔPfPBGD IgG. This laboratory has shown earlier that PfALAD is localized to the apicoplast (12), and PfALAS is localized to the mitochondrion (11). The results presented in Fig. 8 indicate that PfPBGD colocalizes with PfALAD but not with PfALAS, establishing that the native enzyme is localized to the apicoplast in the parasite.

DISCUSSION

In this study, the parasite genome-coded PBGD lacking the hydrophobic N-terminal 64 amino

acids containing the presumptive signal and transit peptide targeting sequences was cloned, and the truncated protein (ΔPfPBGD) was overexpressed in *E. coli*, purified and biochemically characterized. The unique feature is the identification of UROGEN III as the end product, when this recombinant enzyme as well as the native enzyme present in parasite membrane fractions were assayed for porphobilinogen deaminase enzyme activity. Although, Ralph *et al.* (6) and Wilson (8) have alluded to the possible presence of a candidate *hemD* gene (UROS) in *P. falciparum*, so far there has been no report on the expression of this gene or characterization of a separate UROS enzyme in the parasite. The present study indicates that PfPBGD also has UROS activity leading to the formation of UROGEN III. While information on an independent UROS gene and purification of the enzyme is available from different sources such as *E. coli* (33), yeast (34), and the human (35) including its crystal structure (36), there have been no reports on the enzyme or gene from algal and plant sources (37). Interestingly, it has been reported that in *Leptospira interrogans hemC* codes for a bifunctional PBGD/UROS enzyme (38). Further studies are needed to examine whether PfPBGD has segmental homologies to both *hemC/hemD* genes, or the entire protein is required for the manifestation of both the activities as is the case in *Leptospira*. It is also interesting to note that PfPBGD manifests both the activities after heat treatment. It is known that in general while PBGD is heat stable, UROS is heat-sensitive, and heat treatment is included as a step in the purification of PBGD (21, 26).

Another important feature of PfPBGD is its very low catalytic efficiency when compared with the host enzyme, as assessed using the recombinant enzyme. There is almost a 100-fold difference between the catalytic efficiencies of host PBGD and ΔPfPBGD, the k_{cat}/K_m ($M^{-1} s^{-1}$) values being 5.43 and 0.0585, respectively. Although, PfPBGD has all the conserved arginines and other amino acid residues considered essential for the enzyme activity (29–31), there could be other contributory regions, because the parasite enzyme has only around 40% homology with the host red cell enzyme. Studies with ΔPfPBGDL116K mutant enzyme indicate that a change from the native leucine to lysine present in other PBGDs leads to an increase in specific activity by 5-fold. More interestingly, a significant amount of UROGEN I is now seen along with UROGEN III as the product. This would indicate that with increased PBGD activity, the UROS activity of PfPBGD, perhaps, becomes rate-limiting and allows the non-enzymatic cyclization of pre-uroporphyrinogen into UROGEN I.

Sato *et al.* (7) have earlier shown that the N-terminal 65 amino acid residues of PfPBGD fused with GFP is targeted to the apicoplast, when the fusion gene is transfected into the parasite. The present studies with anti-PfPBGD antibodies reveal that the native enzyme is indeed localized to the apicoplast.

Preliminary studies (unpublished) reveal that the parasite cytosol contains imported host red cell PBGD. Earlier studies in this laboratory have demonstrated the import of functional host ALAD (12) and FC (13) into the parasite cytosol. It appears that the parasite genome-coded heme-biosynthetic enzymes are much less efficient than the imported host enzymes and the two pathways in the parasite may be differently compartmentalized (39). These results call for a detailed assessment of the contribution of imported host *Versus* PfPBGD in parasite heme biosynthesis.

REFERENCES

1. Fidock, D. A., Rosenthal, P. J., Croft, S. L., Brun, R., and Nwaka, S. (2004) *Nat. Rev. Drug Discov.* **3,** 509–520
2. Padmanaban, G., Nagaraj, V. A., and Rangarajan, P. N. (2007) *Curr. Sci.* **92,** 1545–1555
3. Surolia, N., and Padmanaban, G. (1992) *Biochem. Biophys. Res. Comm.* **187,** 744–750
4. Bonday, Z. Q., Taketani, S., Gupta, P. D., and Padmanaban, G. (1997) *J. Biol. Chem.* **272,** 21839–21846
5. Gardner, M. J., Shallom, S. J., Carlton, J. M., Salzberg, S. L., Nene, V., Shoaibi, A., Ciecko, A., Lynn, J., Rizzo, M., Weaver, B., Jarrahi, B., Brenner, M., Parvizi, B., Tallon, L., Moazzez, A., Granger, D., Fujii, C., Hansen, C., Pederson, J., Feldblyum, T., Peterson, J., Suh, B., Angiuoli, S., Pertea, M., Allen, J., Selengut, J., White, O., Cummings, L. M., Smith, H. O., Adams, M. D., Venter, J. C., Carucci, D. J., Hoffman, S. L., and Fraser, C. M. (2002) *Nature* **419,** 498–511
6. Ralph, S. A., van Dooren, G. G., Waller, R. F., Crawford, M. J., Fraunholz, M. J., Foth, B. J., Tonkin, C. J., Roos, D. S., and McFadden, G. I. (2004) *Nat. Rev. Microbiol.* **2,** 203–216
7. Sato, S., Clough, B., Coates, L., and Wilson, R. J. (2004) *Protist* **155,** 117–125
8. Wilson, R. J. (2005) *Biol. Rev.* **80,** 129–153
9. van Dooren, G. G., Stimmler, L. M., and McFadden, G. I. (2006) *FEMS Microbiol. Rev.* **30,** 596–630
10. Sato, S., and Wilson, R. J. (2002) *Curr. Genet.* **40,** 391–398
11. Varadharajan, S., Dhanasekaran, S., Bonday, Z. Q., Rangarajan, P. N., and Padmanaban, G. (2002) *Biochem. J.* **367,** 321–327
12. Dhanasekaran, S., Chandra, N. R., Sagar, B. K. C., Rangarajan, P. N., and Padmanaban, G. (2004) *J. Biol. Chem.* **279,** 6934–6942
13. Varadharajan, S., Sagar, B. K. C., Rangarajan, P. N., and Padmanaban, G. (2004) *Biochem. J.* **384,** 429–436
14. Bonday, Z. Q., Dhanasekaran, S., Rangarajan, P. N., and Padmanaban, G. (2000) *Nat. Med.* **6,** 898–903
15. Trager, W., and Jensen, J. B. (1976) *Science* **193,** 673–675
16. Lambros, C., and Vanderberg, J. P. (1979) *J. Parasitol.* **65,** 418–420
17. Fitch, C. D., Chevli, R., Banyal, H., Phillips, G., Pfaller, M. A., and Krogstad, D. J. (1982) *Antimicrob. Agents Chemother.* **21,** 819–822
18. Smythe, E., and Williams, D. C. (1988) *Biochem. J.* **251,** 237–241
19. Lannfelt, L., Wetterberg, L., Lilius, L., Thunnel, S., Jornvall, H., Pavlu, B., Wielburski, A., and Gellerfors, P. (1989) *Scand. J. Clin. Lab. Investig.* **49,** 677–684
20. Weiner, M. P., Costa, G. L., Schoettlin, W., Cline, J., Mathur, E., and Bauer, J. C. (1994) *Gene* **151,** 119–123
21. Jordon, P. M., Thomas, S. D., and Warren, M. J. (1988) *Biochem. J.* **254,** 427–435
22. Lim, C. K., Rideout, J. M., and Wright, D. J. (1983) *Biochem. J.* **211,** 435–438
23. Jordan, P. M., and Warren, M. J. (1987) *FEBS Lett.* **225,** 87–92
24. Sharma, A., and Biswas, S. (2005) *Indian J. Biochem. Biophys.* **42,** 145–151
25. Tonkin, C. J., van Dooren, G. G., Spurck, T. P., Struck, N. S., Good, R. T., Handman, E., Cowman, A. F., and Mc Fadden, G. J. (2004). *Mol. Biochem. Parasitol.* **137,** 13–21
26. Erlandsen, E. J., Jorgensen, P. E., Markussen, S., and Brock, A. (2000) *Scand. J. Clin. Lab. Investig.* **60,** 627–634
27. Jordan, P. M., Burdon, G., Nordlov, H., Schneider, M. M., Pryde, L., and Scott, A. I. (1979). *J. Chem. Soc. Chem. Comm.* 204–205
28. Chartrand, P., Tardif, D., and Sasarman, A. (1979) *J. Gen. Microbiol.* **110,** 61–66
29. Lander, M., Pitt, A. R., Alefounder, P. R., Bardy, D., Abell, C., and Battersby, A. R. (1991) *Biochem. J.* **275,** 447–452

30. Jordan, P. M., and Woodcock, S. C. (1991) *Biochem. J.* **280,** 445–449
31. Louie, G. V., Brownlie, P. D., Lambert, R., Cooper, J. B., Blundell, T. L., Wood, S. P., Warren, M. J., Woodcock, S. C., and Jordan, P. H. (1992) *Nature* **359,** 33–39
32. Miller, A. D., Packman, L. C., Hart, G. J., Alefounder, P. R., Abell, C., and Battersby, A. R. (1989) *Biochem. J.* **262,** 119–124
33. Alwan, A. F., Mqbege, B. I., and Jordan, P. M. (1989) *Biochem. J.* **264,** 397–402
34. Amillet, J. M., and Labbe-Bois, R. (1995) *Yeast* **11,** 419–424

35. Tsai, S. F., Bishop, D. F., and Desnick, R. J. (1988) *Proc. Natl. Acad. Sci. U. S. A.* **85,** 7049–7053
36. Mathews, M. A., Schubert, H. L., Whitby, F. G., Alexander, K. J., Schadick, K., Bergonia, H. A., Phillips, J. D., and Hill, C. P. (2001) *EMBO J.* **20,** 5832–5839
37. Beale, S. I. (1999) *Photosyn. Res.* **60,** 43–73
38. Guegan, R., Camadro, J. M., Girons, I. S., and Picardeau, M. (2003) *Mol. Microbiol.* **49,** 745–754
39. Padmanaban, G., Nagaraj, V. A., and Rangarajan, P. N. (2007) *Trends Biochem. Sci.* **32,** 443–449